HYDROXIDE CO-PRECIPITATION SYNTHESIS OF NMC955 PRECURSOR MATERIAL FOR LITHIUM-ION BATTERIES

Lappeenranta–Lahti University of Technology LUT

Bachelor’s Programme in Chemical Engineering, Bachelor's thesis

2024

Atte Herrala

Examiner: Associate Professor Ekaterina Laakso

ABSTRACT

Lappeenranta–Lahti University of Technology LUT

LUT School of Engineering Sciences

Chemical Engineering

Atte Herrala

Hydroxide co-precipitation synthesis of NMC955 precursor material for lithium-ion batteries

Bachelor's thesis

2024

42 pages, 10 figures, 2 tables

Examiner: Associate Professor Ekaterina Laakso

Keywords: NCM955, cathode material, positive electrode material, Ni-rich cathode, synthesis parameters, synthesis conditions.

The number of batteries used and the performance requirements from them are increasing as the world moves away from fossil fuels towards a more sustainable future. Some of the significant applications for batteries are electric vehicles, energy storage systems and small electronics. Research into battery technologies has been going on for a significant time now and currently lithium-ion batteries are a subject of interest in many fields. Battery materials are one of the main subjects of study and they play a significant role in a battery's performance. While trying to achieve good performance, we are also trying to move away from toxic materials such as cobalt. This has led to one of the most promising materials being Ni-rich transition metal compounds such as NMC. Research is focusing on the methods of creating these compounds through synthesis. The method used and the conditions during it greatly affect the properties of the material. In this thesis previous research is reviewed regarding material compositions and synthesis methods. For NMC955 precursor, one of the favored synthesis methods is hydroxide co-precipitation. The effect of synthesis parameters is studied in a laboratory setting. NMC955 precursors are synthesized and then analyzed using scanning electron microscopy and x-ray diffraction. It is found that a decrease in ammonia concentration corresponds to a smoother particle surface. An increase in stirring speed and synthesis time leads to more uniform round particles. Analysis results from XRD show that most of the structures in the synthesis products are correct. Relatively large crystal size is also confirmed. It is also noted that carefully planning regarding the change in synthesis parameters is vital for accurate results of the synthesis.

TIIVISTELMÄ

Lappeenrannan–Lahden teknillinen yliopisto LUT

LUTin insinööritieteiden tiedekunta

Kemiantekniikka

Atte Herrala

Litiumioniakkujen katodielektrodimateriaalin NMC955 esiasteen hydroksidilaskeutussynteesi

Kemiantekniikan kandidaattiohjelma, Kandidaatintyö

2024

42 sivua, 10 kuvaa, 2 taulukkoa

Tarkastaja: Tutkijaopettaja Ekaterina Laakso

Avainsanat: NCM955, katodimateriaali, positiivinen elektrodi materiaali, korkea nikkeli pitoisuus, synteesi parametrit, synteesi olosuhteet.

Fossiilisista polttoaineista luopuminen kestävämmän tulevaisuuden tavoittelemiseksi on johtanut akkujen tarpeen kasvuun sekä niiden suorituskyvyltä vaaditaan enemmän. Huomattavia akkujen käyttökohteita ovat sähköautot, energiavarastot sekä pienelektroniikka. Akkuteknologian tutkimus on ollut käynnissä jo merkittävän ajan ja tällä hetkellä litium ioni akut ovat keskeisessä asemassa monella saralla. Akkumateriaalit ovat yksi tutkimuksen keskeisiä aihealueita, sillä ne vaikuttavat huomattavasti akkujen suorituskykyyn. Tehokkaampien akkujen lisäksi tavoitteena on luopua haitallisista materiaaleista kuten koboltista. Tämän takia kiinnostavimpia materiaaleja ovat muun muassa suuren nikkeli pitoisuuden materiaalit kuten NMC. Tutkimus keskittyy näiden materiaalien tuottamiseen synteesimetodeilla. Käytetty metodi ja sen olosuhteet vaikuttavat huomattavasti materiaalin ominaisuuksiin. Tässä työssä kootaan yhteen aikaisempaa tutkimusta materiaaleista sekä synteesimetodeista. Yksi paremmista metodeista NMC955:en esiasteen tuottamiseen on hydroksidilaskeutus. Synteesi olosuhteiden vaikutusta tutkitaan laboratorio olosuhteissa. NMC955 esiaste syntetisoidaan ja sitä tutkitaan pyyhkäyselektronimikroskopiaa ja röntgensädediffraktiota käyttäen. Tulosten perusteella todetaan, että ammoniakki konsentraation laskeminen johtaa tasaisempaan partikkelien pintaan. Sekoitusnopeuden sekä synteesiajan nostaminen puolestaan johtaa pyöreämpiin partikkeleihin sekä lisää niiden samankaltaisuutta. XRD tulosten mukaan synteesituotteiden rakenteet ovat halutun laisia. Huomataan myös, että synteesiparametrien muuttamisen tarkka suunnittelu on tärkeää tarkkojen tulosten saamiseksi.

ACKNOWLEDGEMENTS

I would like to thank my supervisor Associate Professor Ekaterina Laakso for providing me with an interesting and challenging subject for this thesis. This has been one of the most intensive learning experiences of the past three years that I have been studying in university.

I would also like to thank Junior Researchers Alisher Kumarov and Yerkezhan Yerkinbekova for their effort in assisting me with the practicalities relating to the laboratory work for this thesis.

Atte Herrala

Lappeenranta 28.3.2024

SYMBOLS AND ABBREVIATIONS

Symbols

kV	Kilovolt
mAh	Milliampere hour
V	Volt
Å	Ångström

Abbreviations

$CoSO_4 \cdot 7H_2O$	Cobalt (II) sulphate heptahydrate
EV	Electric vehicle
LIB	Lithium-ion battery
$LiCoO_2$	Lithium cobalt oxide
$LiFeO_2$	Lithium iron oxide
$LiMnO_2$	Lithium manganese oxide (III)
$LiMn_2O_4$	Lithium manganese oxide (III, IV)
$LiNiO_2$	Lithium nickel oxide
MnOOH	Manganese oxide-hydroxide
MnO_2	Manganese oxide
$MnSO_4 \cdot H_2O$	Manganese (II) sulphate monohydrate
$Mn_3(OH)_4$	Manganese hydroxide
$Mn(OH)_2$	Manganese hydroxide (II)
NaOH	Sodium hydroxide
NCA	Lithiated oxide $LiNi_xCo_yAl_zO_2$

NH_3	Ammonia
NH_4OH	Ammonium hydroxide
NiO	Nickel oxide
$NiSO_4 \cdot 6H_2O$	Nickel (II) sulphate hexahydrate
NMC	Lithiated oxide $LiNí_xMn_yCo_zO_2$
SEM	Scanning Electron Microscope
XRD	X-Ray Diffraction

Table of contents

Figures

Tables

1 Introduction

As the world moves towards a carbon emission-free future, the amount of applications for electricity and thus batteries increase steadily. In recent years this has been shown in the amount of different electric vehicles (EVs) on the market, most notably cars, for which the amount sold in 2021 was 6.6 million vehicles or 10 % of new car sales. This is four times the market share in 2019 (IEA, 2022). While batteries are a popular choice for electricity applications, they are nowhere near perfect with some of the main concerns regarding batteries being the length of their lifecycle and their efficiency. These both can be reduced to being dependent on the properties of the battery with the most prominent ones being capacity retention during cycling, operating voltage, and charge/discharge speed (Malik, Chan and Azimi, 2022). These properties in turn are affected directly by the quality of the materials within the battery and the physical construction of the battery. Research into different designs and structures has reached a point where no significant advances can be made, leaving only material research on the table for the development of better batteries (Noh et al., 2013)

Research into battery materials is constant with many different directions to go to such as different materials, compositions, and production parameters. According to Malik et al., the general material choices are turning towards lithium-ion batteries (LIB's) due to their ideal characteristics for electronics and EVs. For LIB's the characteristics depend on the electrode materials and their composition which is mainly affected by the synthesis conditions. This has led to the development of different methods with the goal of having better control over these conditions which allows more precise production of the materials (Malik, Chan and Azimi, 2022). Research into the different synthesis parameters has been done but the effect varies for different compositions of materials. In nickel-manganese-cobalt materials research can be found on many different compositions, but due to the number of variables during synthesis, more research into them can be used (Entwistle et al., 2022; Malik, Chan and Azimi, 2022). The industry is moving towards materials with high nickel content like NMC955 (Mauler et al., 2022). The effect of synthesis parameters specifically on these materials needs to be studied for optimal production to be achieved in the future.

2 Literature review

All of the current research is based on previously acquired results and general information regarding the topic. This chapter presents some of the information that works as a base for the research, including the experiments listed in this thesis.

2.1 The lithium-ion battery and its mechanisms

An LIB consists of a negative and a positive electrode, which respectively are called the anode and the cathode when referencing a discharging battery. When the battery is charging these roles are reversed. These electrodes consist of 70–95 % of active materials (Monconduit, Croguennec and Dedryvère, 2015). The rest is a binding material and possible additives that are used for enhancing the electrode's electrochemical properties. The electrodes are submerged in a lithium salt solution called the electrolyte. The electrolyte is divided between the electrodes by a separator made of material that allows lithium ions to pass through. Fig. 1 from Warner, 2015 has an illustration of the structure of an LIB.

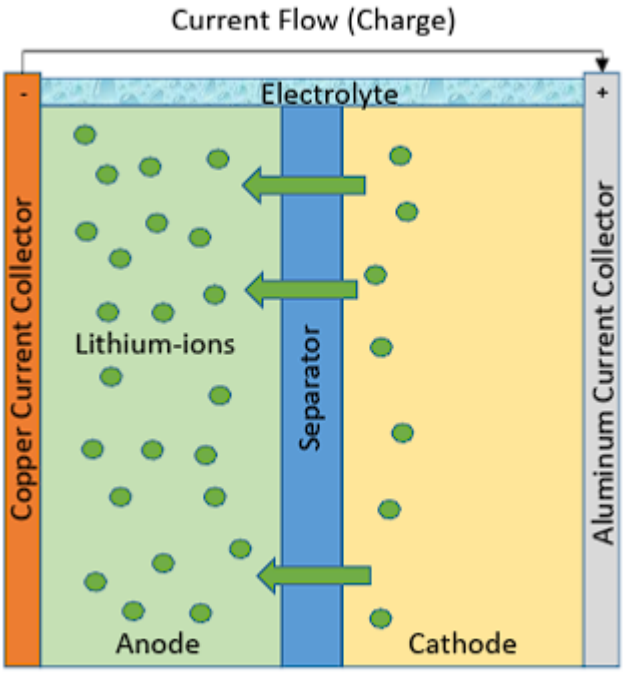

Figure 1. An illustration on the structure of an LIB (Warner, 2015).

The figure also shows the directions in which the ions and current move during charging. When the battery is discharging, these directions are reversed. The reactions happening in the battery are presented below (Akhilash et al., 2021). The M signifies the material used in the cathode.

Cathode: $$LiMO_2 \underset{Discharge}{\overset{Charge}{\rightleftarrows}} Li_{1-x}MO_2 + xLi^+ + xe^-$$

Anode: $$C_6 + xLi^+ + xe^- \underset{Discharge}{\overset{Charge}{\rightleftarrows}} C_6Li_x$$

Overall: $$LiMO_2 + C_6 \underset{Discharge}{\overset{Charge}{\rightleftarrows}} Li_{1-x}CoO_2 + C_6Li_x$$

Some of the applications of LIBs use only one or a few battery cells, such as consumer electronics like smartphones. Larger applications like EVs and electrical grid energy storage system applications utilize larger amounts of cells ranging up to tens of thousands of cells in a system. (Santhanagopalan et al., 2014.)

2.2 Cathode materials for LIB's

The materials suitable to be used in battery electrodes are defined by their electrochemical properties. The main characteristic of the material is its energy density which in determined by its specific capacity and voltage (Akhilash et al., 2021). Other considered characteristics are the material's stability and how it reacts with Li^+ ions (Whittingham, 2004). Nowadays attention is also paid to the material's environmental effects (Akhilash et al., 2021).

2.2.1 $LiMO_2$

The first cathode material used in LIBs was lithium cobalt oxide $LiCoO_2$, which was introduced in 1980 (Akhilash et al., 2021). According to Monconduit et al., it has an operating voltage of 4.2 V and a discharge capacity of 135 mAh g^{-1}. The material is well suited for applications where high operating rates are needed, such as small electronics.

While the capacity of the material isn't optimal, its main drawback comes from cobalt's high price, high toxicity to humans and the environment, ethical problems, and the materials poor thermal stability. These all limit it from being used in applications that require larger batteries such as electric vehicles or energy storage systems. (Monconduit, Croguennec and Dedryvère, 2015).

Another early material is lithium iron oxide $LiFeO_2$. It's also the preferred material due to the abundance of iron and its non-toxicity (Li, J. et al., 2011). According to Akhilash et al. the material comes in multiple different types all which affect its electrochemical properties. Its discharge capacity is anywhere between 120 and 200 mAh g^{-1}. (Akhilash et al., 2021). Operating voltages reach 4.5 V (Sakurai et al., 1997). $LiFeO_2$'s main drawback is its slow Li^+ diffusion causing poor cyclability and limiting its operating rate (Akhilash et al., 2021).

$LiNiO_2$ has the advantage of high lithium extraction giving it a high capacity of around 200 mAh/g (Bianchini et al., 2019). With $LiCoO_2$ and $LiNiO_2$ having similar theoretical capacities of around 275 mAh g^{-1}, it can be seen that nickel-based material uses more of its potential (Akhilash et al., 2021). This combined with its operating voltage of 4.0 V and below makes it a favorable option to $LiCoO_2$ (Dahn et al., 1991). However, $LiNiO_2$ is difficult to synthesize in a specific stoichiometry due to nickel's oxidation states causing changes in the structure (Delmas et al., 1997). Other drawback of the material are poor thermal stability and capacity fading with cycling (Akhilash et al., 2021). These drawbacks have prevented $LiNiO_2$ from being used in commercial applications.

Regarding initial electrochemical performance, the superior transition metal choice is manganese. $LiMnO_2$ has an initial capacity of 250 mAh g^{-1} operating at 4.0 V, but this capacity quickly drops to around 160 mAh g^{-1} (Thackeray, 1997). The drop is caused by a change in the material's structure. A layered structure of $LiMnO_2$ changes to a spinel structure $LiMn_2O_4$ during cycling (Vitins and West, 1997).

While all the above-mentioned materials are suited for use as cathode materials, all of them have significant drawbacks. To counter these drawbacks, research has moved on to mixing these transition metals in different compositions to try and achieve as much of the advantages of each metal while mitigating the drawbacks.

2.2.2 $LiNi_xCo_yAl_{1-x-y}O_2$ (NCA)

Ni-rich compounds have been in focus due to high capacities with low costs (Liu, W. et al., 2015). One of these compounds is NCA, which consists of nickel, cobalt, and aluminum. Addition of cobalt in the material stabilizes the crystallographic structure of nickel by reducing cation mixing (Delmas et al., 1999). Delmas et al. and Cho et al. found that a 1/3 ratio of cobalt to nickel has better capacity retention as well as good rate capability compared to other compositions (Cho, J. et al., 2000; Delmas, Saadoune and Rougier, 1993). Madhavi et al. found that the aluminum in turn improves the material's thermal stability, which is poor with both nickel and cobalt. It also has better capacity and less fading with cycling. The optimal amount of Al is between 5 % and 10 %, while amounts of 20 % and higher present cation mixing and other phase impurities. (Madhavi et al., 2001). Pristine NCA has an initial capacity of 180–199 mAh g^{-1} at 4.3 V depending on the temperature but suffers from quick fading leading to a capacity of around 145 mAh g^{-1} after 100 cycles. This capacity loss can be avoided with the use of additives. (Chen et al., 2018.) During cycling, micro-cracks are also formed in the particles and a NiO-like phase on the surface of the material which leads to degradation of the material causing lower electrochemical properties (Kleiner et al., 2015). A way of preventing this surface degradation is coating the material with inactive metal oxides or metal phosphates, which has been confirmed to prevent the loss of electrochemical performance (Akhilash et al., 2021).

2.2.3 $LiNi_xMn_yCo_{1-x-y}O_2$ (NMC)

Another common composition of transition metals is NMC which consists of nickel, manganese, and cobalt. According to Akhilash et al., these materials have gained interest due to their high discharge capacities. Some of the most common compositions are NMC111, NMC532, NMC622 and NMC811. Research into NMC started from the NMC111 composition which consists of 1/3 of each transition metal. (Akhilash et al., 2021). This material has a capacity of 160 mAh g^{-1} between 2.5 and 4.6 V (Li, D. et al., 2004). It also has very good thermal stability. (Yabuuchi and Ohzuku, 2003). From here research has moved onto Ni-rich compositions due to nickels positive effect on discharge capacity. A general rule of these compounds is that a higher percentage of nickel provides a higher

discharge capacity while decreasing both thermal stability and capacity retention due to approaching $LiNiO_2$. Figure 2. by Noh et al. shows the characteristics of different compositions of NMC.

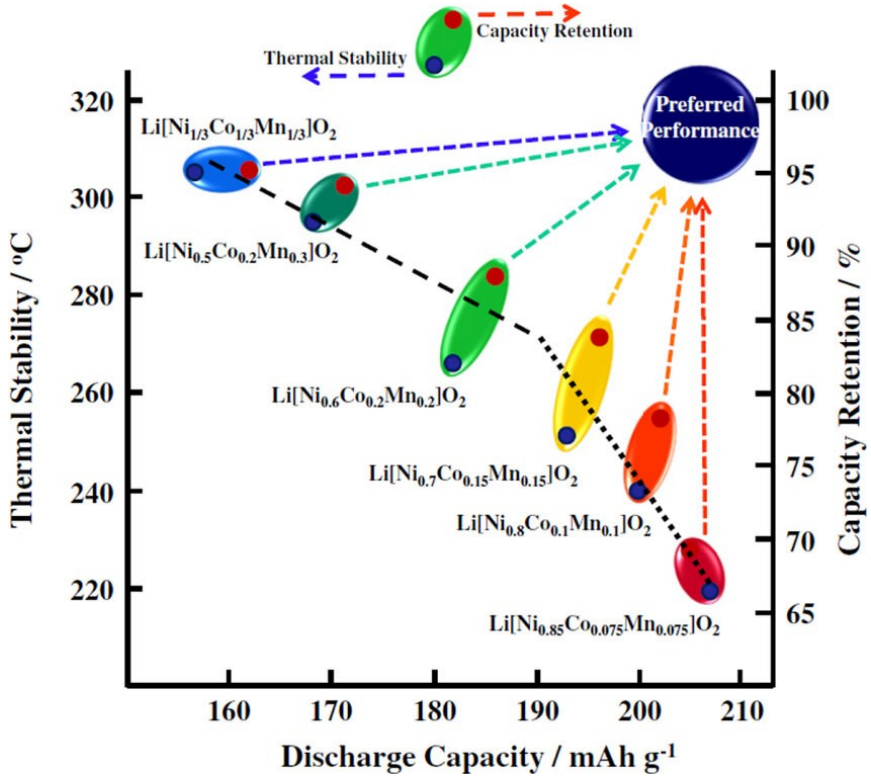

Figure 2. A graph depicting the characteristics of different NMC compositions. Blue dots signify thermal stability, red capacity retention and the black line discharge capacity. (Noh et al,. 2013.)

As the graph shows, discharge capacities for NMC range from NMC111's 160 mAh g^{-1} to almost 210 mAh g^{-1} for $Ni_{0,85}Mn_{0,075}Co_{0,075}$. It's also very apparent how increasing the nickel content affects the materials thermal stability and capacity retention, which both decrease noticeably.

2.2.4 NMC955

NMC955 consists of 90 % nickel, 5 % manganese and 5 % cobalt. This composition is sought after in the industry. This is due to the aforementioned high capacity achieved with high

nickel content and decreased raw material costs due to 21 % higher cell density and better efficiency. The material still requires research and improvement as it has problems with thermal stability and performance decay. (Mauler et al., 2022).

2.3 Synthesis methods for NMC through precursors

NMC precursors are acquired by some mean of synthesis through the reaction shown below. The source of the transition metals varies by method and can sometimes be chosen, but it affects the component Z that forms into the precursor, which is the material without the lithium in it. For instance, when using sulphates, the component is $(OH)_2$ and when using carbonates, it's CO_3. Some of the other possible sources are acetates and metal chlorides (Malik, Chan and Azimi, 2022).

$$Ni^{2+}{}_x + Mn^{2+}{}_y + Co^{2+}{}_{1-x-y} + 2Z^- \rightarrow Ni_xMn_yCo_{1-x-y}Z_2$$

$$Li^+ + Ni_xMn_yCo_{1-x-y}Z + O_2 \rightarrow Li\left[Ni_xMn_yCo_{1-x-y}\right]O_2$$

The lithium is added in a sintering/calcination process, where the materials are heated to a high temperature in an atmosphere where oxygen is present. This leads to different phases of the precursor transforming into the final product. (Malik, Chan and Azimi, 2022.) Over time methods using different chemicals in different conditions have been developed and naturally the older synthesis methods have had more research done on them. Industrial applications tend to gravitate towards these methods while research of newer methods is showing promising results. The end product's quality is affected by the synthesis parameters such as pH, temperature, precipitation time, stirring rate and the chelating agent's type and concentration (Malik, Chan and Azimi, 2022). Different methods provide different means of varying effectiveness to control these parameters. Next are presented some of the most common synthesis methods. Their advantages and drawbacks are also discussed.

2.3.1 Co-precipitation method

Co-precipitation is the most common method of synthesis for NMC and its precursors because it is a simple and easily scalable process, making it suitable for laboratory scale research as well as industrial applications (Ahaliabadeh et al., 2022). There are three

common kinds of co-precipitation methods: hydroxide-, carbonate-, and oxalate co-precipitation (Malik, Chan and Azimi, 2022).

The hydroxide co-precipitation method is based on the reaction of transition metal sulphates, for NMC these are nickel, manganese, and cobalt sulphates. A stoichiometric amount based on the decided composition of the material of these sulphates are hydrated, and ammonia is used as a complexing agent. According to Entwistle et al., the reaction requires a high pH value of around 11 for optimal formation of particles, so some kind of hydroxide is used to maintain this pH. Sodium hydroxide is a widely chosen chemical for this as it's cheaper in high purities compared to other hydroxides (Entwistle et al., 2022). The ammonia concentration's effect in hydroxide co-precipitation was studied by Deng et al. who did experiments with five different concentrations. They came to the conclusion that a concentration of 0,35 mol L^{-1} resulted in the best formation of particles due to the ammonia preventing phase separation and allowing a more homogenous mix of the transition-metal hydroxides (Deng et al., 2010). Hydroxide co-precipitation allows good control of particle size and is very economical considering the quality of the finished material (Yang et al., 2015). On the other hand, it has drawbacks that increase the method's complexity. There are limitations regarding the manganese concentration of the finished product that require extra steps during the synthesis. Because of the usage of sulphates, an inert atmosphere is required for the synthesis. This needs to be done to prevent impurities from forming due to unwanted oxidation of the manganese. Instead of the forming of $Mn(OH)_2$ the Mn^{2+} ions can bind with extra oxygen forming MnOOH, MnO_2 and Mn_3O_4 particles that have worse electrochemical properties and causes a different stoichiometry than originally planned (Wang, D. et al., 2011).

The requirement for inert atmosphere can be avoided with carbonate co-precipitation. The only difference compared to hydroxide co-precipitation is the source of the transition metals. Instead of sulphates, the method uses a carbonate salt $Ni_xMn_yCo_{1-x-y}CO_3$. According to Cho et al., the carbonate salt locks the valence state of the Mn to 2+ removing the need for an inert atmosphere. Another advantage of carbonate co-precipitation is a decreased optimal pH value with it dropping from hydroxide co-precipitation's 11 to 8 (Cho, T. H. et al., 2005). While this fixes some of the problems, carbonate co-precipitation has its own challenges. When using ammonia as a chelating agent, there can be noticeable differences in stoichiometric compositions between the planned and final products. This is due to the

ammonia slowing down the rate of the nickels deposition (Zhu, Z. et al., 2013). According to Malik, Chan and Azimi, another problem comes from the carbonate causing increased porosity of the secondary particles. The increased porosity causes the product to be more fragile, which in turn can lead to cracking during sintering. It also causes larger particles which might not be usable in electrode materials due to poor electrochemical properties (Malik, Chan and Azimi, 2022).

The third most common co-precipitation method is oxalate co-precipitation. For co-precipitation agent, oxalic acid is used in sodium hydroxide's place (Malik, Chan and Azimi, 2022). This leads to the transition metals forming oxalates which in turn has the same effect as using carbonate salts as a source for the metals. It locks the manganese ion's valence state to 2+ thus eliminating the need for an inert atmosphere (Wang, D. et al., 2013). One of the advantages of oxalate co-precipitation over carbonate co-precipitation is that it produces high quality particles regardless of the desired composition of transition metals (Dong et al., 2019). However, while good quality, according to Wang et al. the produced particles can have different crystallographic structures depending on the synthesis conditions. This can lead to different phases forming in the final product, which leads to worse electrochemical properties (Wang, D. et al., 2011). The biggest challenges with oxalate co-precipitations stem from the fact that oxalate salts have relatively poor solubility in water (Malik, Chan and Azimi, 2022). This leads to a limited synthesis rate compared to hydroxide and carbonate co-precipitation (Wang, D. et al., 2011).

All three co-precipitation methods are viable ways of synthesizing NMC and its precursors. Which method to use depends on the purpose of synthesizing and use case of the final product. Hydroxide method has a good synthesizing rate and good control of particle formation apart from high manganese concentrations while requiring a more complex setup and having rougher environmental parameters. The carbonate method is a more neutral and simple way of synthetization while trading it for a slightly unreliable particle composition especially in high nickel concentrations. Oxalate method solves the biggest challenges of the previous two methods while having a slower synthesis rate and requiring careful planning of synthesis parameters to obtain homogenous particle structures. These properties make hydroxide co-precipitation favorable for industrial applications while carbonate and oxalate co-precipitations are in their current state fore suitable for laboratory and research purposes.

As also pointed out by Malik et al., future research should focus on improving these two methods (Malik, Chan and Azimi, 2022).

2.3.2 Sol-gel method

Like co-precipitation, the sol-gel method also uses the transition metals in stoichiometric amounts as starting ingredients. In this method they are either nitrate hydrates or acetate hydrates that are dissolved in distilled water. As a chelating agent the method uses citric acid mixed with lithium nitrate or acetate. The solution's pH is maintained at 8 with ammonium hydroxide and the method requires a temperature of around 80 °C. Magnetic stirring is used to achieve a transparent viscous solution which is dried at 120 °C to obtain the precursor material. (Malik, Chan and Azimi, 2022.)

The Sol-gel method has multiple advantages, especially regarding the structure of the final product. According to Klein, Aparicio and Damay, the method gives good control over the stoichiometry and particle size. It also has mild synthesis conditions, and the product has good crystallographic structure. (Klein, Aparicio and Damay, 2016.) Having small uniform particles with good crystallographic structure provides the material good electrochemical properties, which are in this case better than most solid-state reactions (Liu, H. et al., 2004). On the other hand, the process is complex, time-consuming and causes moderate environmental contamination, which all lead to high energy consumption and production costs (Zhao et al., 2020).

Even though the method has been around for a long time, the effect of synthesis parameters except for chelating agent are not well studied. Many different chelating agents have been investigated and citric acid is the most common one due to it being cheap, environmentally friendly and one of the most effective agents. (Malik, Chan and Azimi, 2022.) A study by Li et al. found that a most effective chelating agent would be glucose though it's not used due to a requirement of three times the amount of glucose compared to citric acid (Li, W. et al., 2020; Malik, Chan and Azimi, 2022).

2.3.3 Hydrothermal method

One of the most prominent synthesis methods for NMC and its precursors in current research is the hydrothermal method. This is because it has slight advantages over the other more common methods such as co-precipitation (Malik, Chan and Azimi, 2022). As described by Wang et al., the method begins the same way as before mentioned methods with mixing stoichiometric quantities of transition metals and dissolving them in distilled water. The metals are in acetate hydrate form, ethylene glycol is used as chelating agent, and oxalic acid is used to adjust the pH of the solution. A Teflon-lined stainless-steel autoclave filled to 80 % at 200 °C for 6-18 hours is used to obtain the precursor material. The material is then separated and washed with distilled water and ethanol in a centrifuge and dried at 80 °C. (Wang, L. et al., 2016.) According to Malik et al., slightly different temperatures and autoclave duration are possible, as well as using nitrate hydrate forms of the transition metals or ethanolamine as a chelating agent. When working towards a finished NMC material, lithium is added to the precursor, though it can also be added to the stoichiometric mix of transition metals at the start of the synthesis. The solvent used to dissolve the transition metals can also be changed to an organic solvent like ethylene glycol. When this is done the name of the method is changed to hydro/solvothermal or solvothermal respective of whether the change is partial or complete. (Malik, Chan and Azimi, 2022.)

The reason why this method is popular is due to its ability to synthesize homogenous material with better than other methods' electrochemical properties like capacity, stability, and rate capability (Pan et al., 2013). As researched by Shi, Chen and Chen, an interesting characteristic of the hydrothermal method is that in addition to synthesizing material from the individual transition metals, it can also be used as a treatment method alongside other synthesis methods like co-precipitation. This way the quality of the material can be improved, or used material can be regenerated by using it as the starting material for the synthesis. This works by improving the crystallographic structure of the material leading to enhanced electrochemical properties. (Shi, Chen and Chen, 2018.) The method doesn't have any inherent problems with it though the long time required by the autoclave limits its industrial applications (Malik, Chan and Azimi, 2022).

2.3.4 Spray pyrolysis method

One of the most favorable methods for industrial applications is spray pyrolysis method. Many forms of transition metal salts can be used as starting materials, such as acetates, chlorides, nitrates, lactates, citrates and oxalates. The salts are dissolved in distilled water and the solution is made into an aerosol in an atomizer. This aerosol is then heated somewhere below 1000 °C in a reactor. The temperature is chosen according to preferred particle size and distribution. At this temperature each droplet in the aerosol goes through a series of reactions such as solvent vaporization, solute precipitation, diffusion, decomposition and agglomeration. The exiting particles are collected with a filter. The synthesis process is continuous, so residence time in the reactor greatly affects the particle size. While there is no lower boundary to the particle size, production rate of particles under 50 nm gets so low that other methods should be considered. A well-known problem with the method is the formation of hollow particles which increases with transition metal salt concentration in the aerosol. A thin crust can be formed on the outer edge of a particle blocking the solvent from permeating it. This leads to pressure buildup inside the particle and eventually the particle shatters when the pressure is released. (Zhu, Y. et al., 2017.)

Spray pyrolysis is unique in the way it provides uniform atomic-level mixing and narrow particle size distribution (Zhu, Y. et al., 2017). The method also has high production rate due to low residence time in the reactor, high purity and no need for extra steps after synthesis for good quality material (Lengyel et al., 2014). The method is also environmentally friendly because of no liquid waste or need for recycling. These advantages of the method have led to it being widely used in addition to batteries in industrial applications such as fuel cells, superconductors, thin film depositions and photocatalysts. On the other hand, the equipment required is expensive and the method is complex, which is why it’s not commonly used in laboratory research. (Malik, Chan and Azimi, 2022.)

2.3.5 Solid-state method

When research into transition metal oxides as cathode material began in 1980’s, one the first methods of synthesis was solid-state method (Mizushima et al., 1980). A carefully measured stoichiometric amounts of transition metal powders are used as starting ingredients. Instead

of using a solvent the powders are mixed mechanically for a few hours. The mix is then heated for 4-6 h at 500 °C, then 8-15 h at 1000 °C, or in one step of 10-25 h at 1000 °C. The method allows to obtain a very precise stoichiometry of the final product, though as a downside the long hold times at high temperatures combined with the mechanical mixing make the solid-state method very energy intensive. (Malik, Chan and Azimi, 2022.) Long exposure to high temperatures also affects the composition of the final product. The conditions cause a lack of oxygen in the reaction atmosphere leading to a decrease in nickel's oxidation state causing decomposition of the transition metal. This leads to worse electrochemical properties, though the effects can be minimized by using an oxygenated atmosphere during the process. (Yamada, Fujiwara and Kanda, 1995.) Possibly the biggest drawback compared to other methods is the lack of control over particle properties like morphology, which mainly affect the electrochemical performance and energy density of the material (Malik, Chan and Azimi, 2022).

2.3.6 Combustion method

Like many of the other methods, combustion method starts with dissolving a stoichiometric amount of transition metal salts into distilled water and into this solution a fuel is added (Patoux and Doeff, 2004). Among used fuels are nitrate/urea mixture, sucrose, glycine/urea mixture and hexamethylenetetramine (Malik, Chan and Azimi, 2022). The solution is then dried and after that heated to a temperature at which the used fuel has its ignition point. The rise in temperature, especially when the fuel ignites, causes nucleation in the materials which leads to the formation of NMC particles. (Ahn et al., 2014.)

The method is simple and cost-effective due to a short reaction time, simple equipment and no need for external energy (Patoux and Doeff, 2004). The chemical composition, particle shape and size are easy to control and optimize (Malik, Chan and Azimi, 2022). The method is mainly limited by its large particle size and a possibility of impurities in the product due to incomplete combustion (Xu et al., 2018).

2.3.7 Choosing a method for NMC955 precursors

To summarize, all the methods and their advantages and drawbacks are presented in table 1. After, it is discussed which method would be the most suited for producing NMC955 precursors.

Table 1. A summary of the synthesis methods' advantages and drawbacks.

Method	**Advantages**	**Drawbacks**
Hydroxide co-precipitation	Good particle control Good cost/quality ratio	Inert atmosphere requirement Fairly complex setup
Carbonate co-precipitation	Neutral conditions No need for controlled atmosphere	Inaccuracies in stoichiometry with high nickel concentrations Increased porosity of secondary particles
Oxalate co-precipitation	High quality products regardless of stoichiometry	Low synthesis rate Possible phase separation
Sol-Gel	Good control of stoichiometry and particle size Uniform particles with good structure	Complex and time-consuming process Environmental contamination High energy and production costs
Hydro-/Solvothermal	Homogenous material with good properties	Complex equipment
Spray pyrolysis	Atomic-level mixing Narrow size distribution High production rate and purity	Complex and expensive equipment Possibility of hollow particles which end up blown apart
Solid-state	Precise stoichiometry of final product	Long hold time Energy intensive Lack of control over particle morphology and other properties
Combustion	Simple and cost-effective Easy control of particle shape and size	Large particle size Possibility of impurities in final product

Because of NMC955's high nickel concentration, carbonate co-precipitation is not a good choice due to the inaccuracies in stoichiometry. Because of the small amounts of manganese and cobalt, the precise stoichiometry provided by solid-state method would be important as even small deviations can cause either metal's amount to drop too low for acceptable performance of the material. Because of today's attempts to be more environmentally friendly, sol-gel and solid-state methods are not ideal. Oxalate co-precipitation, spray pyrolysis and combustion method all have drawbacks regarding the quality of the final product's particles, which all from a commercial standpoint make the material not suitable for use as a standardized quality is important. The choice is between hydroxide co-precipitation and hydro-/solvothermal method. Both of these have good quality products at good costs. Both methods are good choices for producing NMC955 and the chosen method depends on preference, and other research and use conditions of the final product.

3 Materials and methods

This chapter presents the used synthesis process of NMC955 precursor. Subjects included are preparation of materials, co-precipitation synthesis process and product analysis methods. A total of 5 rounds of synthesis were conducted with varying conditions to examine the particles formed under different conditions.

3.1 Material preparation

NMC955 precursor $Ni_{0,9}Mn_{0,05}Co_{0,05}(OH)_2$ was synthesized using co-precipitation method. The source of the transition metals was sulphates. Molar amounts of 0,009 mol of nickel (II) sulphate hexahydrate ($NiSO_4 \cdot 6H_2O$, 98+ %, Thermo scientific), 0,00054 mol of manganese (II) sulphate monohydrate ($MnSO_4 \cdot H_2O$, ≥98 %, MERCK) and 0,00054 mol of cobalt (II) sulphate heptahydrate ($CoSO_4 \cdot 7H_2O$, ≥99 %, MERCK) were measured using an analytical balance. The sulphates were then dissolved in an amount of pure water shown in table 2. for each round of synthesis.

A 25 % ammonium hydroxide solution (NH_4OH, 25 % extra pure, Thermo scientific) was used as a source of NH_3 for a chelating agent. For each round of synthesis, a volume according to a NH_3 concentration shown in table 2. was measured using a measuring glass. For controlling the synthesis pH, a 1 M NaOH solution was prepared by dissolving NaOH crystals to pure water in a volumetric flask.

In table 2. are shown the different conditions used in each of the 5 synthesis rounds.

Table 2. Synthesis conditions for each run.

Run #	V/H_2O (ml)	c/NiMnCo (mol/L)	c/NH_3 (mol/L)	pH	Temperature (°C)	Stirring speed (rpm)	Time (h)
1	100	0,09	1,64	10	60	300	6
2	100	0,11	0,07	10	50	300	7
3	75	0,14	0,55	10	50	300	7
4	75	0,14	0,55	10	50	800	12
5	35	0,29	0,86	11	50	800	7

The synthesis conditions were changed based on the results of previous runs and research found in literature.

3.2 Synthesis equipment

The equipment used was a reaction flask with three necks, a glass container with enough depth to house the reaction flask halfway, a magnetic stirrer with a thermoregulator (Velp Scientifica, Arex-6 Digital Pro), a pH meter with integrated temperature sensor (Mettler Toledo, FiveEasy) and a nitrogen gas supply for providing an inert atmosphere into the flask. The equipment was constructed in a fume hood. The synthesis equipment setup is shown in figure 3.

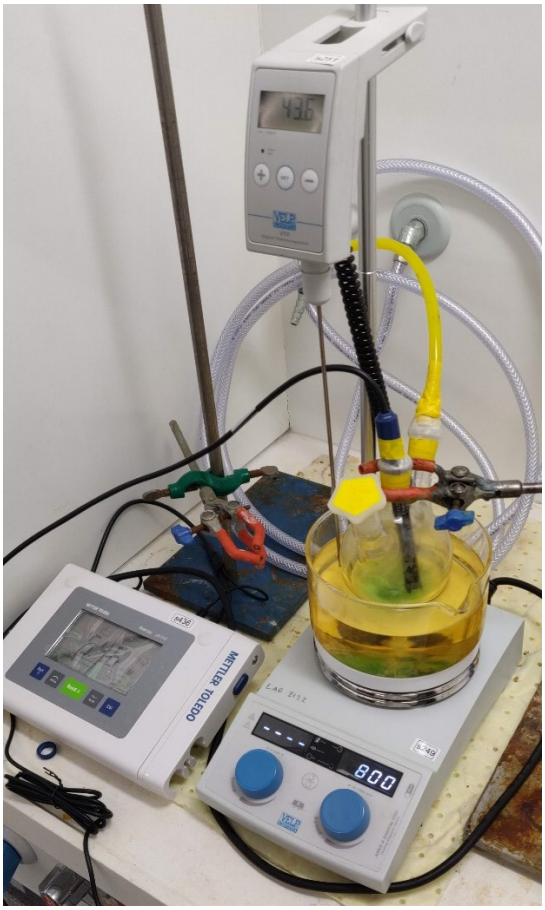

Figure 3. The synthesis equipment setup.

As the reaction requires heat, the reaction flask was 1/3 submerged in heating oil heated by the magnetic stirrer's heating plate. Into the reaction flask were inserted the pH meter and a nozzle for the nitrogen gas supply. The nitrogen supply is through the clear/yellow tube from the back of the fume hood. The necks used for these were sealed using parafilm and plastic tape. The third neck was used to insert the chemicals and sealed with a cap. The sealing was done to prevent evaporation and the entering of air into the flask. Magnets for stirring were inserted into the reaction flask as well as the oil bath to provide better heat transfer from the heating plate to the reaction flask. The heating plates monitoring probe was inserted into the heating oil and the temperature in the reaction flask was monitored through the pH meter's integrated temperature sensor. The nitrogen flow was controlled through a pressure valve on the fume hood.

3.3 Synthesis and analysis process

The synthesis process began by inserting the transition metal solution into the reaction flask. Then, nitrogen flow, heating and stirring were turned on, after which the NH_4OH solution was added. For runs 1–3., the solution was added right after the heat and stirring were turned on and for runs 4. and 5. the solution was added once the transition metal solution had reached the desired synthesis temperature. The pH of the solution inside the reaction flask was kept at the desired value by adding drops of 1M NaOH solution. Pictures taken during run 5. are shown in figure 4.

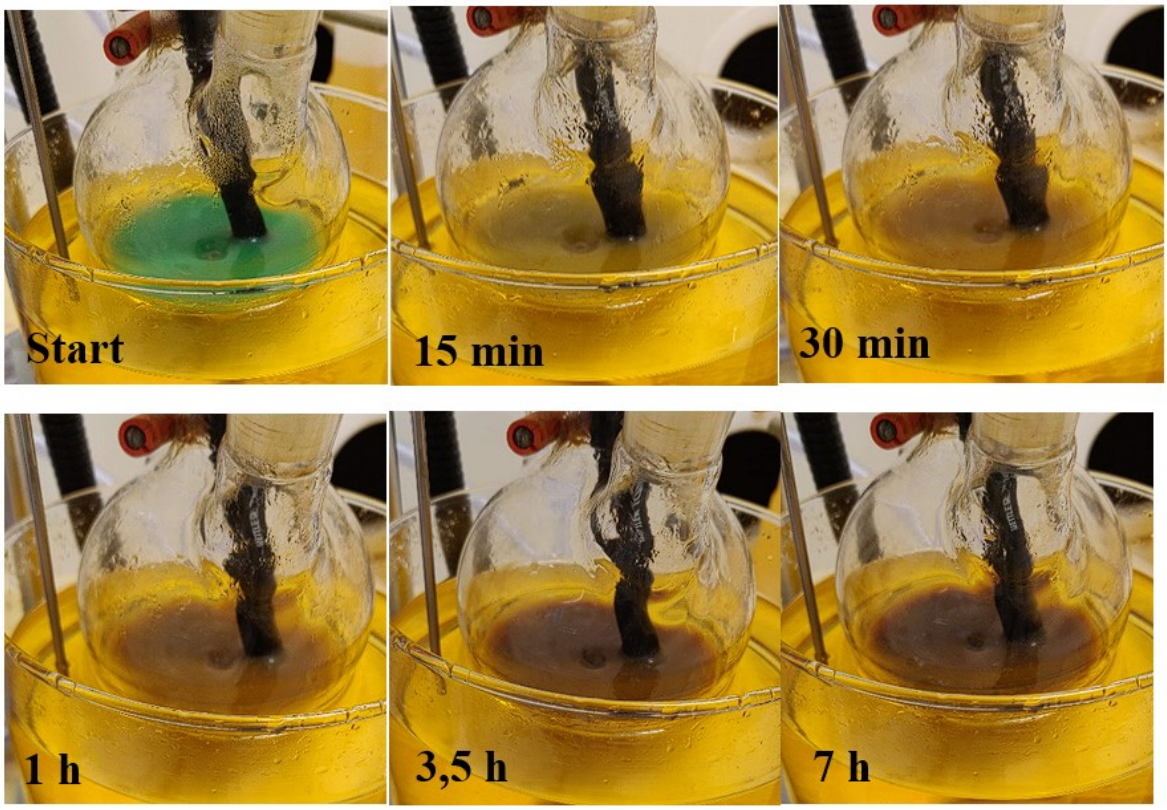

Figure 4. Pictures showing the progression of the synthesis during run 5.

The transition metal solution is a turquoise translucent liquid. When NH_4OH was added, the solution turned opaque. When the reaction starts, the solution starts to quickly turn brown and by the end it's a dark brown color. After the synthesis had been going on for the desired time, the solution from the reaction flask was filtered to remove excess liquid. The remaining

solid was then washed 5 times with pure water in a centrifuge for 5 minutes at 3000 rpm. The solid was then dried at 60 °C overnight.

For analysis, the obtained solid sample was ground in a mortar to obtain a fine dust. A scanning electron microscope (HITACHI, SU3500) was used for analysis of the formed particles. Pictures were taken at an operating voltage of 5 kV at magnifications between x100–x5000, 10 kV at magnifications between x500–x2000 and 15 kV at magnification of x2000. Samples from runs 1. and 5. were analyzed using x-ray diffraction to characterize the particles' crystalline structure. Measurements were conducted in room temperature using two x-ray diffractometers. An instrument (Bruker B8 Advance) with Cu $K_{\alpha 1}$ type radiation (λ = 1.5406 Å) produced by a copper sealed tube x-ray source was used. Diffractograms were collected in a 2θ range of 10–90° at 0.026° intervals with a scan rate of 0.033° per second. An operating voltage of 45 kV and a current of 40 mA were used.

4 Results and discussion

This chapter focuses on presenting the results of synthesizing NMC955 precursors using hydroxide co-precipitation. The goal of this study was to obtain particles with round shape and narrow size distribution while also observing the effect of synthesis conditions on the particles.

4.1 Synthesized material and its particle shape and size

Each synthesis run yielded a dark solid compound. Pictures of these compounds are presented in figure 5.

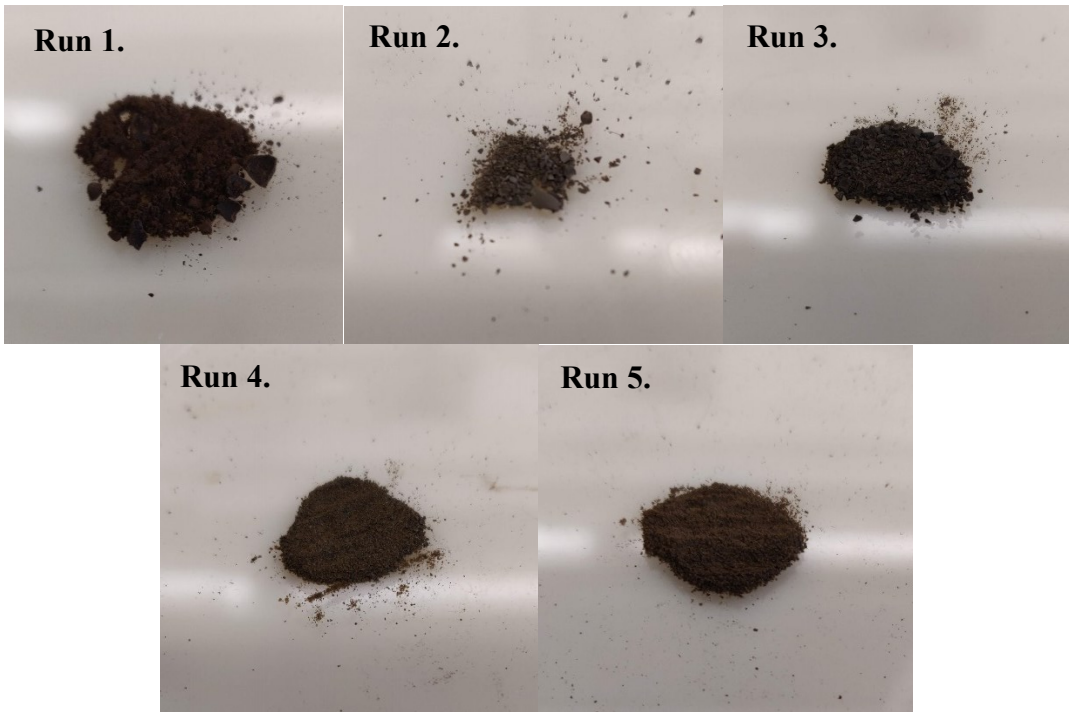

Figure 5. Pictures of each of the five synthesis runs' products.

Particle sizes visible in these pictures are not indicative of the actual secondary particle size. SEM images from these samples showing a larger number of particles are displayed in figure 6. Average secondary particle size can be approximated using the measuring scale provided by the SEM to the images.

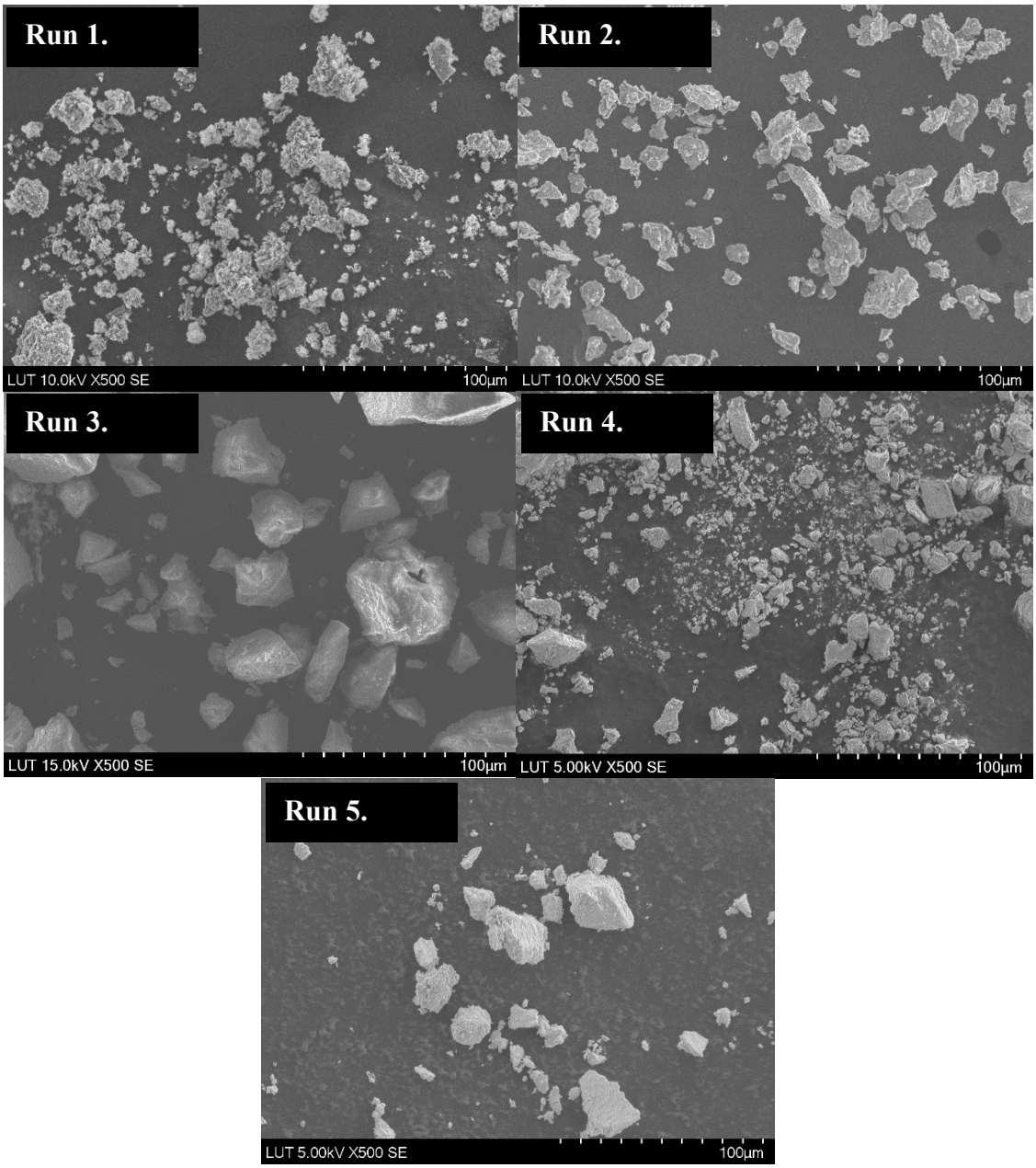

Figure 6. SEM images with a larger number of particles from each of the five runs.

The secondary particle size ranges from 50 µm to 200 µm as can be seen from the images. These are quite large for NMC secondary particles, as a more common secondary particle size is around 10 µm as demonstrated by Noh et al. and Barai et al. (Barai et al., 2019; Noh et al., 2013.) It can also be seen that the particles are not very round but instead have sharp edges. NMC primary particles should resemble a ball and while secondary particles might

be more irregular shapes, they should still have round edges because of the shape of the primary particles (Malik, Chan and Azimi, 2022).

4.2 Effect of synthesis conditions on particle structure

Varying synthesis conditions were used to obtain different particles. This subchapter presents these results and discusses the effects of the synthesis parameters.

4.2.1 Effect of NH_3 concentration

Ammonia concentrations of 1,64 M, 0,86 M, 0,55 M and 0,07 M were used during synthesis. SEM images of the results are displayed in figure 7.

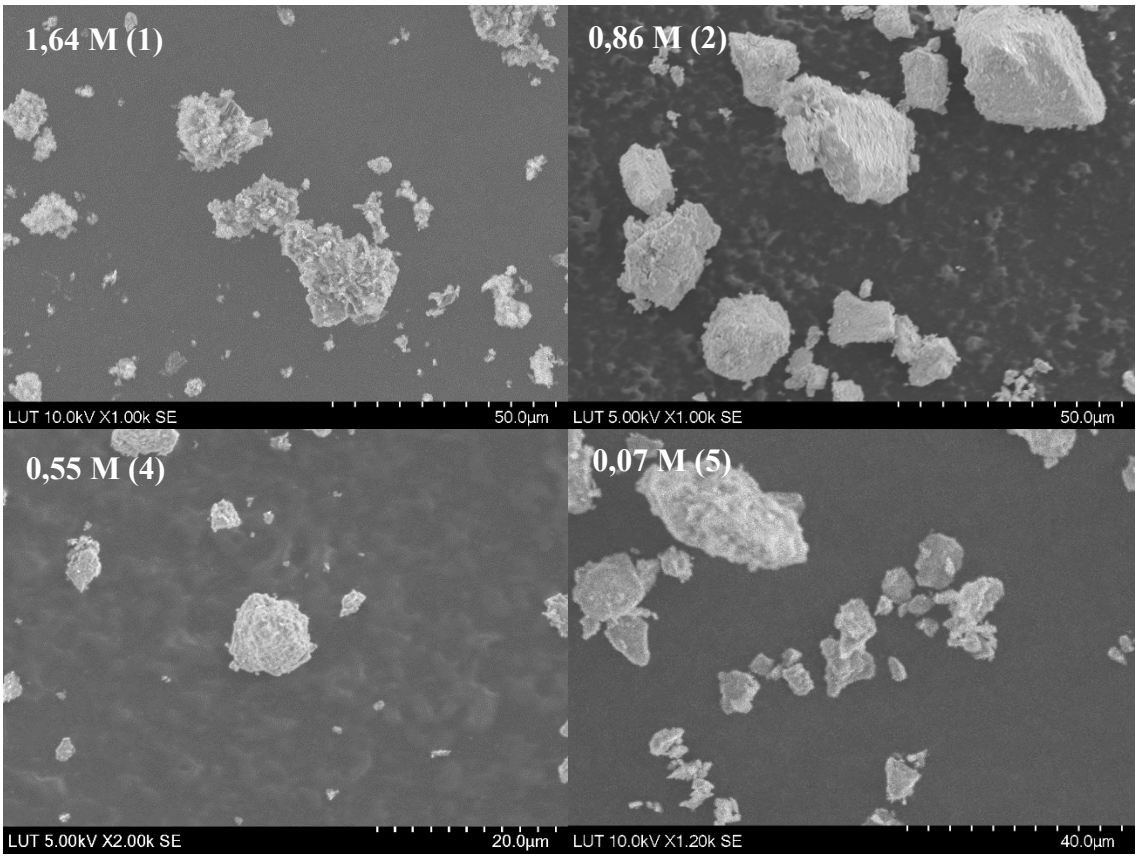

Figure 7. SEM images with particles from runs 1, 2, 4 and 5.

A decrease in ammonia concentration leads to a smoother surface on the particles with the most notable change between 1,64 M and 0,86 M concentrations. According to Barai et al. a lower concentration of NH_3 leads to a decrease in particle size, but this can't be confirmed from these results as the variance in particle size for one run is too large (Barai et al., 2019).

Figure 8. Shows pictures of run 1. and 2.'s compounds from each end of the NH_3 concentration spectrum with 1,64 mol L^{-1} and 0,07 mol L^{-1} concentrations.

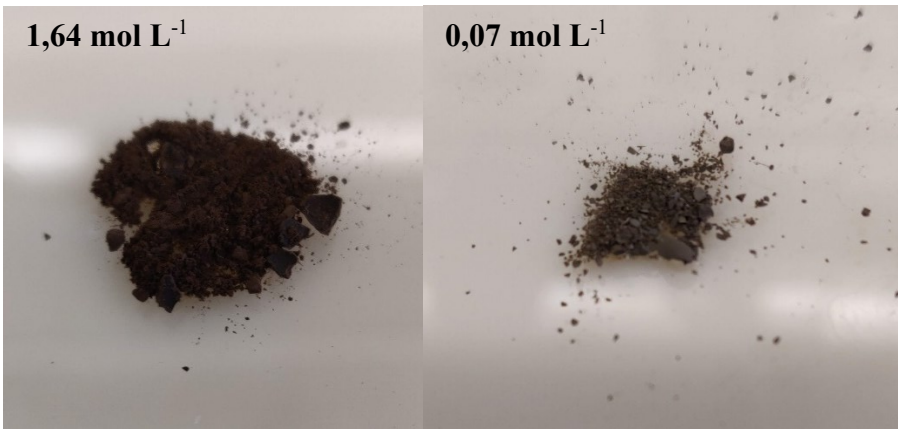

Figure 8. Pictures of compounds from runs 1. and 2. with NH_3 concentrations of 1,64 mol L^{-1} and 0,07 mol L^{-1} respectively.

As can be seen, a higher ammonia concentration during synthesis causes the resulting compound to be darker in color, while a lower concentration retains more of the turquoise hue that comes from the nickel sulphate. This is likely caused by the oxidation state of the nickel.

4.2.2 Effect of synthesis time and stirring speed

Runs 3. and 4. had the same synthesis conditions apart from run 3. being 7 hours with a stirring speed of 300 rpm and run 4. being 12 hours with a stirring speed of 800 rpm. SEM images from these two runs are shown in figure 9.

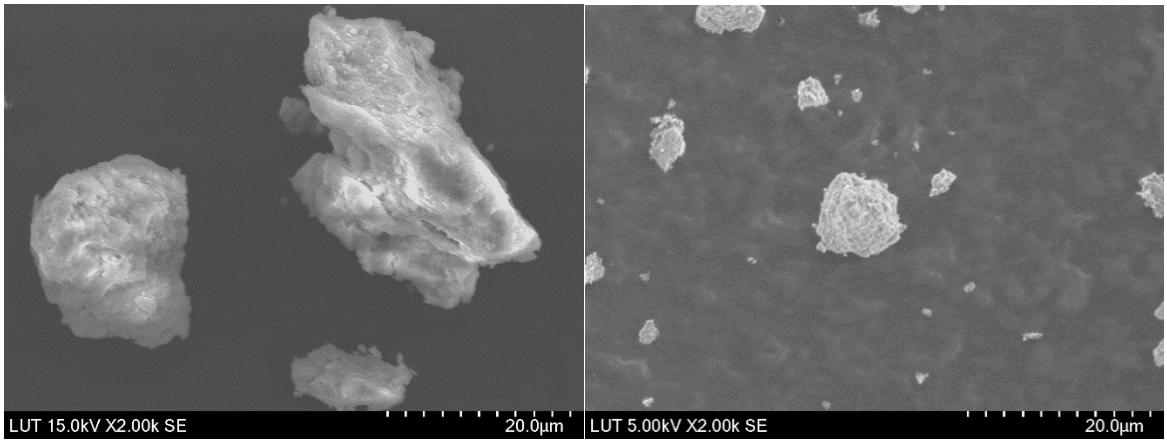

Figure 9. SEM images from run 3. with 7-hour time and a stirring speed of 300 rpm and run 4. with 12-hour time and a stirring speed of 800 rpm.

It appears that a longer synthesis time and a higher stirring speed allow for more uniform and round particles. Particles from run 4. don't have most of the rough edges that particles from run 3. have, while also the particles are more like each other. This would follow what Deng et al. found in their study of reaction time and what Ren et al. found in their study of stirring speed (Deng et al., 2010; Ren et al., 2017). These are speculative conclusions, because the change in multiple parameters at once doesn't allow for confirmation of the cause of these changes in the particles.

4.2.3 Effect of other synthesis parameters

While other synthesis parameters such as transition metal concentration, pH value and temperature were slightly varied during the five runs, the effects of these parameters can't accurately enough be observed from the acquired SEM images. This is because of time constraints during this study that led to need of making multiple changes to the synthesis parameters between runs in order to try and achieve the best quality particles.

4.2.4 Results of XRD analysis

In figure 10. is a graph obtained from XRD analysis of samples from runs 1. and 5.

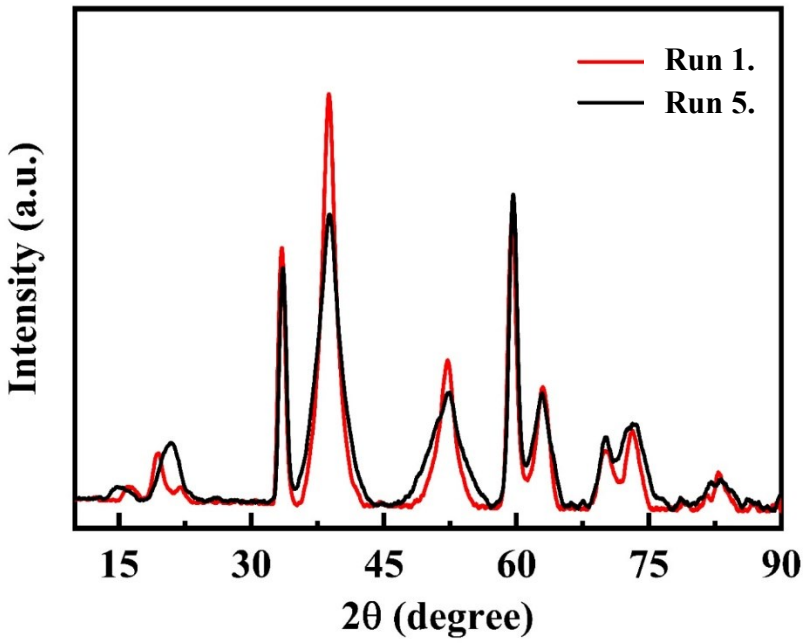

Figure 10. XRD patterns from samples obtained from runs 1. and 5.

The graph can be analysed to verify that the compound consists of the correct transition metal hydroxides. For $Ni(OH)_2$, spikes at 2θ values of 20.9°, 33.6°, 38.8° and 52.4° are in line with graphs JCPDS No.14-0117 and JCPDS No.38-0715, which confirms the existence of the general structure. $Ni(OH)_2$ can exist in two different phases called α and β. The graphs for both runs line up with graphs for β-$Ni(OH)_2$ and α-$Ni(OH)_2$. This suggests the nickel is a two phase mixture, though the amount of α-$Ni(OH)_2$ indicates that a majority of the material is β-$Ni(OH)_2$ with small impurities of α-$Ni(OH)_2$. β-$Ni(OH)_2$ structure is indicative of a stacking fault disorder with increased electrochemical activity compared to the α-$Ni(OH)_2$ structure, which has a general structure disorder. (Hall et al., 2015.) As for $Mn(OH)_2$, it is most likely replaced by Mn_2O_3 structures instead as the spikes line up better with its XRD graph JCPDS No.73-1826. This suggests that the synthesis atmosphere isn't inert and contains oxygen leading to oxidation of Mn^{2+} ions during synthesis. This would lead to the Mn replacing the Ni and Co in the crystal lattice due to a change in its ionic radius. Spikes relating to $Co(OH)_2$ (JCPDS No.30-0443) are visible at 2θ values of 20.9°, 38.8° and 62.9°. The exact changes in these structures or their amounts can't be deducted from this graph as the spikes for the different structures overlap significantly. The spikes are very wide at low intensities which signifies that the particles with these structures are quite large. This aligns with the data obtained from the SEM pictures.

4.3 Possible ways of developing the study method

Time constraints combined with the large amount of synthesis parameters and their effects on the particles led to the analysis results having a large number of different changes which made drawing accurate conclusions difficult. Continuing from the results of this study, it would be recommended to limit the changes in parameters from one run to another to achieve more precise results on their effects.

5 Conclusions

A study into the synthesis of NMC955 precursor using hydroxide co-precipitation was conducted. Five synthesis runs were done with different synthesis parameters. A solid compound representing the desired material was obtained and analyzed with SEM. Particle shape does resemble previous results from research found in literature, though the obtained results could be improved upon. Same goes for particle size, which was quite large compared to expectations. Regarding the effect of ammonia concentration, a higher concentration leads to sharper particles. A lower concentration in turn yields smoother particles. According to literature, a lower concentration should also lead to a smaller particle size, but this couldn't be confirmed from the SEM images due to a high variance in particle size. The effect of synthesis time and stirring speed was also examined. A longer time and higher stirring speed appeared to have a positive effect on the formation of particles as these led to more uniform and round particles. These conclusions were speculative as changing multiple parameters at once didn't allow for accurate examination of their effects. As for other synthesis parameters, due to time constraints the parameters couldn't be varied in a way that would have allowed for their effects to be analyzed. Instead of this, trying to synthesize particles of a better shape and size was favored. XRD results from 2 runs show slight changes in the crystallographic structures of the material and confirm the findings from SEM regarding a large particle size. For future research into this subject, it is recommended to limit the scope of examined parameters relative to the available resources.

References

Ahaliabadeh Z, Kong X, Fedorovskaya E and Kallio T (2022) Extensive comparison of doping and coating strategies for Ni-rich positive electrode materials. *Journal of Power Sources* 540: 231633.

Ahn W, Lim SN, Jung K, Yeon S, Kim K, Song HS and Shin K (2014) Combustion-synthesized LiNi0.6Mn0.2Co0.2O2 as cathode material for lithium ion batteries. *Journal of Alloys and Compounds* 609: 143-149.

Akhilash M, Salini PS, John B and Mercy TD (2021) A journey through layered cathode materials for lithium ion cells – From lithium cobalt oxide to lithium-rich transition metal oxides. *Journal of Alloys and Compounds* 869: 159239.

Barai P, Feng Z, Kondo H and Srinivasan V (2019) Multiscale Computational Model for Particle Size Evolution during Coprecipitation of Li-Ion Battery Cathode Precursors. *The Journal of Physical Chemistry.B* 123(15): 3291-3303.

Bianchini M, Roca-Ayats M, Hartmann P, Brezesinski T and Janek J (2019) There and Back Again—The Journey of LiNiO2 as a Cathode Active Material. *Angewandte Chemie (International Ed.)* 58(31): 10434-10458.

Chen T, Li X, Wang H, Yan X, Wang L, Deng B, Ge W and Qu M (2018) The effect of gradient boracic polyanion-doping on structure, morphology, and cycling performance of Ni-rich LiNi0.8Co0.15Al0.05O2 cathode material. *Journal of Power Sources* 374: 1-11.

Cho J, Jung H, Park Y, Kim G and Lim HS (2000) Electrochemical Properties and Thermal Stability of Li[sub a]Ni[sub 1−x]CO[sub x]O[sub 2] Cathode Materials. *Journal of the Electrochemical Society* 147(1): 15.

Cho TH, Park SM, Yoshio M, Hirai T and Hideshima Y (2005) Effect of synthesis condition on the structural and electrochemical properties of Li[Ni1/3Mn1/3Co1/3]O2 prepared by carbonate co-precipitation method. *Journal of Power Sources* 142(1-2): 306-312.

Dahn JR, Von Sacken U, Juzkow MW and Al-Janaby H (1991) Rechargeable LiNiO2/carbon cells. *Journal of the Electrochemical Society* 138(8): 2207-2211.

Delmas C, Saadoune I and Rougier A (1993) The cycling properties of the LixNi1−yCoyO2 electrode. *Journal of Power Sources* 44(1): 595-602.

Delmas C, Ménétrier M, Croguennec L, Saadoune I, Rougier A, Pouillerie C, Prado G, Grüne M and Fournès L (1999) An overview of the Li(Ni,M)O2 systems: syntheses, structures and properties. *Electrochimica Acta* 45(1): 243-253.

Delmas C, Peres JP, Rougier A, Demourgues A, Weill F, Chadwick A, Broussely M, Perton F, Biensan P and Willmann P (1997) On the behavior of the LixNiO2 system : an electrochemical and structural overview. *Journal of Power Sources* 68(1): 120-125.

Deng C, Zhang S, Fu BL, Yang SY and Ma L (2010) Synthetic optimization of nanostructured Li[Ni 1/3Mn 1/3Co 1/3]O 2 cathode material prepared by hydroxide coprecipitation at 273 K. *Journal of Alloys and Compounds* 496(1): 521-527.

Dong H, Gardner E, Barron AF and Koenig GM (2019) Apparent activation energy of multicomponent transition metal oxalates to probe synthesis of battery precursor materials. *Powder Technology* 354: 158-164.

Entwistle T, Sanchez-Perez E, Murray GJ, Anthonisamy N and Cussen SA (2022) Co-precipitation synthesis of nickel-rich cathodes for Li-ion batteries. *Energy Reports* 8: 67-73.

Hall DS, Lockwood DJ, Bock C and MacDougall BR (2015) Nickel hydroxides and related materials: a review of their structures, synthesis and properties. *Proc. R. Soc. A*(471:20140792).

IEA (2022) *Global EV Outlook 2022.* Available at: https://www.iea.org/reports/global-ev-outlook-2022.

Klein LC, Aparicio M and Damay F, (2016) *Sol–Gel Processing for Battery and Fuel Cell Applications.* In: Klein L, Aparicio M and Jitianu A (eds) Handbook of Sol-Gel Science and Technology. : Springer International Publishing.

Kleiner K, Melke J, Merz M, Jakes P, Nagel P, Schuppler S, Liebau V and Ehrenberg H (2015) Unraveling the Degradation Process of LiNi0.8Co0.15Al0.05O2 Electrodes in Commercial Lithium Ion Batteries by Electronic Structure Investigations. *ACS Applied Materials & Interfaces* 7(35): 19589-19600.

Lengyel M, Atlas G, Elhassid D, Luo PY, Zhang X, Belharouak I and Axelbaum RL (2014) Effects of synthesis conditions on the physical and electrochemical properties of Li sub(1.2)Mn sub(0.54)Ni sub(0.13)Co sub(0.13)O sub(2) prepared by spray pyrolysis. *Journal of Power Sources* 262: 286-296.

Li D, Muta T, Zhang L, Yoshio M and Noguchi H (2004) Effect of synthesis method on the electrochemical performance of LiNi1/3Mn1/3Co1/3O2. *Journal of Power Sources* 132(1-2): 150-155.

Li J, Li J, Luo J, Wang L and He X (2011) Recent Advances in the LiFeO2-based Materials for Li-ion Batteries. *International Journal of Electrochemical Science* 6(5): 1550-1561.

Li W, Yao L, Zhang X, Lang W, Si J, Yang J and Li L (2020) The effect of chelating agent on synthesis and electrochemical properties of LiNi0.6Co0.2Mn0.2O2. *SN Applied Sciences* 2(4): 554.

Liu H, Wu YP, Rahm E, Holze R and Wu HQ (2004) Cathode materials for lithium ion batteries prepared by sol-gel methods. *Journal of Solid State Electrochemistry* 8(7): 450-466.

Liu W, Oh P, Liu X, Lee M, Cho W, Chae S, Kim Y and Cho J (2015) Nickel-Rich Layered Lithium Transition-Metal Oxide for High-Energy Lithium-Ion Batteries. *Angewandte Chemie (International Ed.)* 54(15): 4440-4457.

Madhavi S, Subba Rao GV, Chowdari BVR and Li SFY (2001) Effect of aluminium doping on cathodic behaviour of LiNi 0.7Co 0.3O 2. *Journal of Power Sources* 93(1): 156-162.

Malik M, Chan KH and Azimi G (2022) Review on the synthesis of LiNixMnyCo1-x-yO2 (NMC) cathodes for lithium-ion batteries. *Materials Today Energy* 28: 101066.

Mauler L, Lou X, Duffner F and Leker J (2022) Technological innovation vs. tightening raw material markets: falling battery costs put at risk. *Energy Advances* 1(3): 136-145.

Mizushima K, Jones PC, Wiseman PJ and Goodenough JB (1980) LixCoO2 (0<x<-1): A new cathode material for batteries of high energy density. *Materials Research Bulletin* 15(6): 783-789.

Monconduit L, Croguennec L and Dedryvère R, (2015) *Electrodes for Li-Ion Batteries. Volume 2, Materials, Mechanisms and Performance.* London, England ;: ISTE.

Noh H, Youn S, Yoon CS and Sun Y (2013) Comparison of the structural and electrochemical properties of layered Li[NixCoyMnz]O2 (x = 1/3, 0.5, 0.6, 0.7, 0.8 and 0.85) cathode material for lithium-ion batteries. *Journal of Power Sources* 233: 121-130.

Pan C, Banks CE, Song W, Wang C, Chen Q and Ji X (2013) Recent development of LiNixCoyMnzO2: Impact of micro/nano structures for imparting improvements in lithium batteries. *Transactions of Nonferrous Metals Society of China* 23(1): 108-119.

Patoux Sand Doeff MM (2004) Direct synthesis of LiNi 1/3Co 1/3Mn 1/3O 2 from nitrate precursors. *Electrochemistry Communications* 6(8): 767-772.

Ren D, Shen Y, Yang Y, Shen L, Levin BDA, Yu Y, Muller DA and Abruña H,D. (2017) Systematic Optimization of Battery Materials: Key Parameter Optimization for the Scalable Synthesis of Uniform, High-Energy, and High Stability LiNi0.6Mn0.2Co0.2O2 Cathode Material for Lithium-Ion Batteries. *ACS Applied Materials & Interfaces* 9(41): 35811-35819.

Sakurai Y, Arai H, Okada S and Yamaki J (1997) Low temperature synthesis and electrochemical characteristics of LiFeO2 cathodes. *Journal of Power Sources* 68(2): 711-715.

Santhanagopalan S, Kim G, Keyers M, Pesaran AA, Smith K and Neubauer J, (2014) *Design and Analysis of Large Lithium-Ion Battery Systems.* Boston: Artech House.

Shi Y, Chen G and Chen Z (2018) Effective regeneration of LiCoO 2 from spent lithium-ion batteries: a direct approach towards high-performance active particles. *Green Chemistry : An International Journal and Green Chemistry Resource : GC* 20(4): 851-862.

Thackeray MM (1997) Manganese oxides for lithium batteries. *Progress in Solid State Chemistry* 25(1): 1-71.

Vitins Gand West K (1997) Lithium intercalation into layered LiMnO2. *Journal of the Electrochemical Society* 144(8): 2587-2592.

Wang D, Belharouak I, Zhou G and Amine K (2013) Synthesis of Lithium and Manganese-Rich Cathode Materials via an Oxalate Co-Precipitation Method. *Journal of the Electrochemical Society* 160(5): A3108-A3112.

Wang D, Belharouak I, Koenig GM, Zhou G and Amine K (2011) Growth mechanism of Ni0.3Mn0.7CO3 precursor for high capacity Li-ion battery cathodes. *Journal of Materials Chemistry* 21(25): 9290-9295.

Wang L, Wu B, Mu D, Liu X, Peng Y, Xu H, Liu Q, Gai L and Wu F (2016) Single-crystal LiNi0.6Co0.2Mn0.2O2 as high performance cathode materials for Li-ion batteries. *Journal of Alloys and Compounds* 674: 360-367.

Whittingham MS (2004) Lithium Batteries and Cathode Materials. *Chemical Reviews* 104(10): 4271-4302.

Xu L, Zhou F, Liu B, Zhou H, Zhang Q, Kong J and Wang Q (2018) Progress in Preparation and Modification of LiNi0.6Mn0.2Co0.2O2 Cathode Material for High Energy Density Li-Ion Batteries. *International Journal of Electrochemistry* 2018: 1-12.

Yabuuchi Nand Ohzuku T (2003) Novel lithium insertion material of LiCo1/3Ni1/3Mn1/3O2 for advanced lithium-ion batteries. *Journal of Power Sources* 119-121: 171-174.

Yamada S, Fujiwara M and Kanda M (1995) Synthesis and properties of LiNiO2 as cathode material for secondary batteries. *Journal of Power Sources* 54(2): 209-213.

Yang Y, Xu S, Xie M, He Y, Huang G and Yang Y (2015) Growth mechanisms for spherical mixed hydroxide agglomerates prepared by co-precipitation method: A case of Ni1/3Co1/3Mn1/3(OH)2. *Journal of Alloys and Compounds* 619: 846-853.

Zhao Y, Yuan X, Jiang L, Wen J, Wang H, Guan R, Zhang J and Zeng G (2020) Regeneration and reutilization of cathode materials from spent lithium-ion batteries. *Chemical Engineering Journal (Lausanne, Switzerland : 1996)* 383: 123089.

Zhu Y, Choi SH, Fan X, Shin J, Ma Z, Zachariah MR, Choi JW and Wang C (2017) Recent Progress on Spray Pyrolysis for High Performance Electrode Materials in Lithium and Sodium Rechargeable Batteries. *Advanced Energy Materials* 7(7): np-n/a.

Zhu Z, Zhang D, Yan H, Li W and Qilu (2013) Precise preparation of high performance spherical hierarchical LiNi0.5Mn1.5O4 for 5 V lithium ion secondary batteries. *Journal of Materials Chemistry.A, Materials for Energy and Sustainability* 1(18): 5492.